Supplementary Material

In previous work, we demonstrated that 3' → 5' RNA decay followed by scavenger decapping of the resulting cap was very active in our translation extracts (1). In contrast, direct mRNA decapping occurred at very low levels in the translation extracts, and thus 5' → 3' decay played a very minor role in mRNA decay compared to the 3' → 5' RNA decay pathway. To rule out that the mutations in blocks 1 or 3 led to differential RNA decapping of RNA that might contribute to the differences in translation observed, we examined the rate of decay of 5' monophosphate RNAs (the products of RNA decapping) and compared the amounts of decapped RNAs derived from wild type or mutant SL mRNAs that accumulated during translation in the extracts (see Materials and Methods). 5' monophosphate RNAs were significantly less stable than TMG-capped RNAs in the extracts indicating that decapped RNAs are not likely to accumulate in the extracts (Supplementary Figure 2A). In addition, comparison of the wild-type and mutant RNAs at different time points during translation did not show any differences in the levels of decapped or 5' monophosphate RNAs for these RNAs during the translation reactions (Supplementary Figure 2B). Overall, these data suggest that differential mRNA decapping of wild-type vs mutant SL 1 and 3 is not an explanation for the reduction in translation observed for the mutations in the SLs.

References

1. **Cohen, L. S., C. Mikhli, C. Friedman, M. Jankowska-Anyszka, J. Stepinski, E. Darzynkiewicz, and R. E. Davis.** 2004. Nematode m7GpppG and m3(2,2,7)GpppG decapping: activities in Ascaris embryos and characterization of C. elegans scavenger DcpS. RNA **10:**1609-24.
2. **Lall, S., C. C. Friedman, M. Jankowska-Anyszka, J. Stepinski, E. Darzynkiewicz, and R. E. Davis.** 2004. Contribution of trans-splicing, 5' -leader length, cap-poly(A) synergism, and initiation factors to nematode translation in an Ascaris suum embryo cell-free system. J Biol Chem **279:**45573-85.
3. **Merino, E. J., K. A. Wilkinson, J. L. Coughlan, and K. M. Weeks.** 2005. RNA structure analysis at single nucleotide resolution by selective 2'-hydroxyl acylation and primer extension (SHAPE). J Am Chem Soc **127:**4223-31.
4. **Wilkinson, K. A., E. J. Merino, and K. M. Weeks.** 2006. Selective 2'-hydroxyl acylation analyzed by primer extension (SHAPE): quantitative RNA structure analysis at single nucleotide resolution. Nat Protoc **1:**1610-6.

Supplementary Figures

Supplementary Figure 1. eIF4G protein alignment. Identical residues are shaded grey and similar residues are white with black shading. Ascaris is *Ascaris suum* (ACX37244), Brugia is *Brugia malayi*

(XP_001895525, parasitic nematode), C. elegans is *Caenorhabditis elegans* (NP_001022259), bee is *Apis mellifera (*XP_393239), human is *Homo sapiens* eIF4GI (Q04637), and wheat is *Triticum aestivum (*Q03387). Boxed and arrowed regions indicate domains in the human eIF4GI.

Supplemental Figure 2. 5' monophosphate RNAs decay faster than capped RNAs and levels of uncapped RNAs are not different between the WT SL and SL Mut-3. A). Decay of monophosphate mRNA compared with capped RNAs during Ascaris cell-free translation. GMP RNAs were primed with GMP and thus contain a 5'-monophosphate. RNAs were analyzed as described in Figure 1 C. **B).** Assay for presence of decapped, 5'-monophosphate RNAs during translation. RNAs were isolated at the illustrated time points and treated with Terminator enzyme. Terminator enzyme degrades only 5'-monophosphate RNAs (not 5' capped, triphosphate, or diphosphate RNAs)(Epicentre, Madison, WI). The plots illustrate the amount of remaining RNA during translation that is resistant to terminator enzyme (e.g., capped RNA). Note that WT SL and the Mut-3 SL RNAs do not show significant differences in the degree of uncapped RNAs.

Supplemental Figure 3. Spliced leader sequences required for efficient translation. A). Multiple nucleotides within block 1 of the SL contribute to translation of TMG-capped RNAs. **B).** Multiple nucleotides within block 3 of the SL contribute to translation of TMG-capped RNAs. **Raw data for spacing analysis normalized in Figure 3. C).** Insertion mutations were designed with compensating deletions after the SL (e.g., SL-G+2N and -2N) to account for changes in the length of the 5' UTR on translation. The actual decrease in translation from the insertions (SL-G+XN) is greater when deletion mutations (-XN) are considered. These data were used to present normalized values in Figure 6 by dividing the translation level of the "SL-G+XN" value by the "-XN" value

Supplementary Figure 4. Mutations in block 3 of the spliced leader results in increased flexibility in both blocks 1 and 3 suggesting residues within these blocks interact. A). TMG-capped 64 nucleotide WT SL and GGGU MUT 3 RNAs were analyzed using SHAPE (3, 4). Mutations in nucleotides 10 – 13 (Block 3) caused increased flexibility in those nucleotides as well as near the cap, nucleotides 2 – 4 (Block 1). Marked in red are the nucleotides in blocks 1 and 3. **B).** Quantitation of accessibility changes illustrated in A. Gels illustrated in A were subjected to phosphoimager analysis. Experiments were carried out as described in the Materials and Methods.

Supplementary Figure 5. m^7GTP-sepharose treatment of Ascaris extracts reduces eIF4G and eIF4E. Ascaris translation extract was treated with m^7GTP-sepharose and the amount of various proteins removed from the extract determined by Western Blotting. Antibodies to the Ascaris proteins were generated to full-length eIf4E-3, a truncated form of eIF4G, and peptides derived from the N-terminus of Ascaris eIF4E-1 and eIF4E-4 (Davis et al, unpublished).

Supplementary Figure 6. SL affects translation at the initiation step. A). Translation time course for WT SL and GGGT Mut-3 RNA. **B).** Translation time course for WT SL and GGGT Mut-3 RNA illustrating the linear phase of translation. **C).** Sucrose gradients of Ascaris Extract with WT SL and GGGT Mut-3 RNA. Experiments were carried out as described in the Materials and Methods.

Supplementary Figure 7. The SL stem loop does not increase Ascaris eIF4E/4G's affinity for TMG-capped RNAs. A). Ascaris eIF4E/G complex has the same affinity for the TMG-capped wild-type SL, stem-loop mutant, and compensatory stem-loop mutant. The figures illustrate the surface plasmon resonanse responses and residuals obtained for binding of varying concentrations of eIF4E/G to different immobilized RNAs. The burnt orange lines show best fit used for analysis. These data were used to calculate values shown in Table 1. Concentrations of eFI4E/G used were 1.73 nM, 3.45 nM, 6.9 nM, 13.8 nM, 27.6 nM. **B).** Translation inhibition assay using trimethylguanosine cap analog. Note that the cap analog does not differentially affect translation of the mRNAs. **C).** Ultraviolet light crosslinking of recombinant Ascaris eIF4E-3 to universally labeled RNAs. Experiments were performed as previously described (2).

Supplementary Figure 8. The C. elegans SL2 and hybrid SLs between SL1 and C. elegans SL2 variants support translation of a TMG-capped RNA. A). Analysis of translation of C. elegans SL2, hybrid spliced leaders, and other SL variants. **B).** Translation of Trichinella spliced leaders. Experiments were carried out as described in Figure 1. Blue sequences represent SL1 nucleotides, orange SL2 nucleotides, and green and purple nucleotides are variant in alternate SL2-like leaders

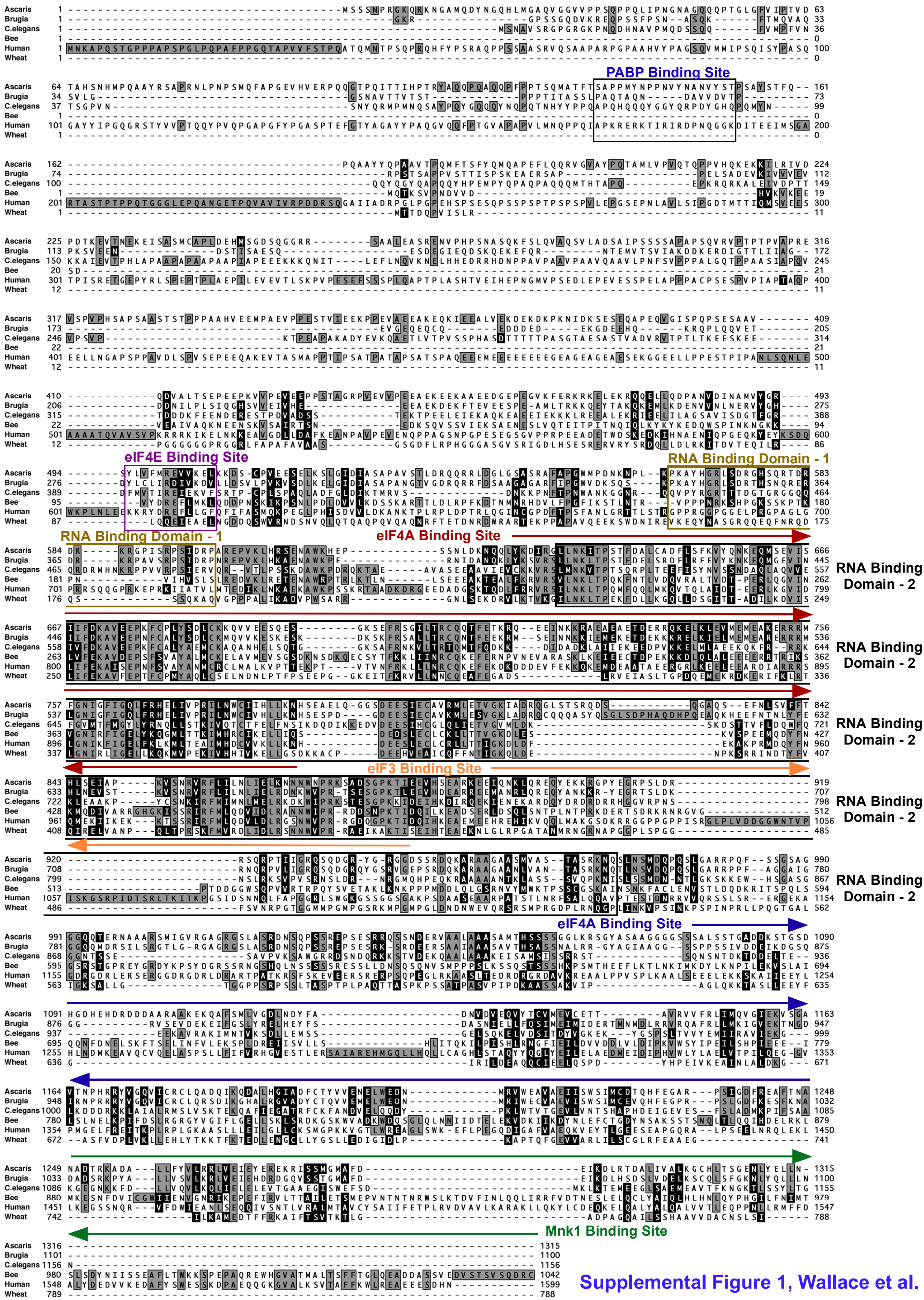

Supplemental Figure 1, Wallace et al.

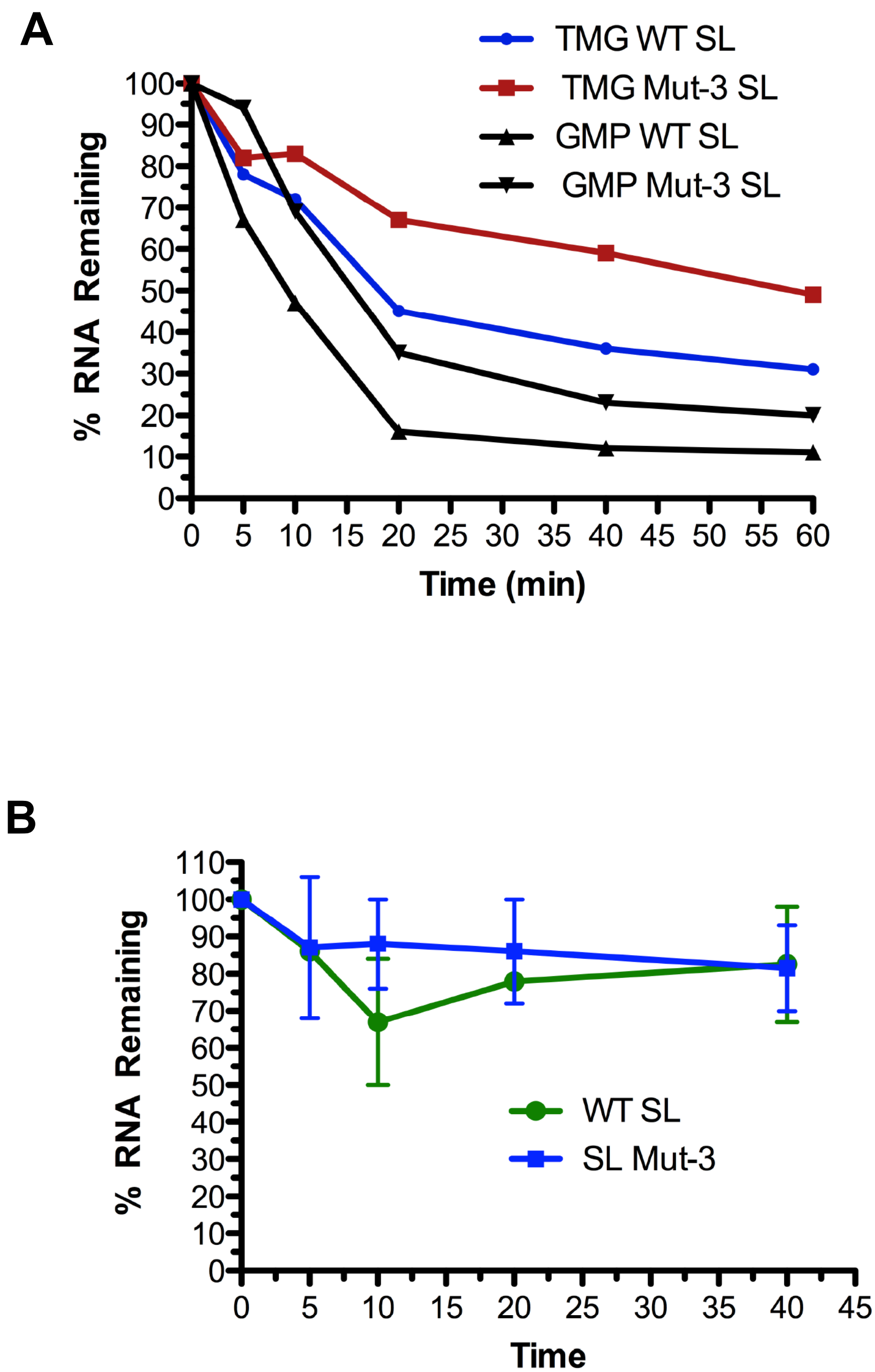

Supplemental Figure 2, Wallace et al.

Supplemental Figure 3, Wallace et al.

A

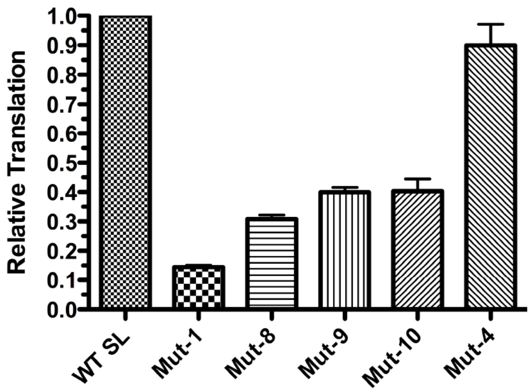


```
                         SL                    ATG
WT      GGTTTAATTACCCAAGTTTGAGGGCTAGCCACCATGACTTC
Mut-1   GNNNNAATTACCCAAGTTTGAGGGCTAGCCACCATGACTTC
Mut-8   GNNTTAATTACCCAAGTTTGAGGGCTAGCCACCATGACTTC
Mut-9   GGNNTAATTACCCAAGTTTGAGGGCTAGCCACCATGACTTC
Mut-10  GGTNNAATTACCCAAGTTTGAGGGCTAGCCACCATGACTTC
Mut-4   GGTTTAATTACCCANNNNTGAGGGCTAGCCACCATGACTTC
```

B

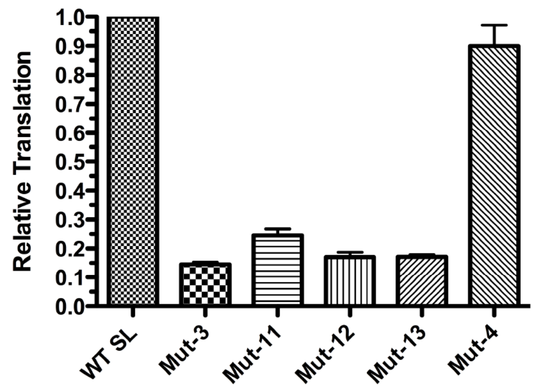


```
                         SL                    AUG
WT      GGUUUAAUUACCCAAGUUUGAGGGCUAGCCACCAUGACUUC
Mut-3   GGUUUAAUUNNNNAAGUUUGAGGGCUAGCCACCAUGACUUC
Mut-11  GGUUUAAUUNNCCAAGUUUGAGGGCUAGCCACCAUGACUUC
Mut-12  GGUUUAAUUANNCAAGUUUGAGGGCUAGCCACCAUGACUUC
Mut-13  GGUUUAAUUACNNAAGUUUGAGGGCUAGCCACCAUGACUUC
Mut-4   GGUUUAAUUACCCANNNNUGAGGGCUAGCCACCAUGACUUC
```

C

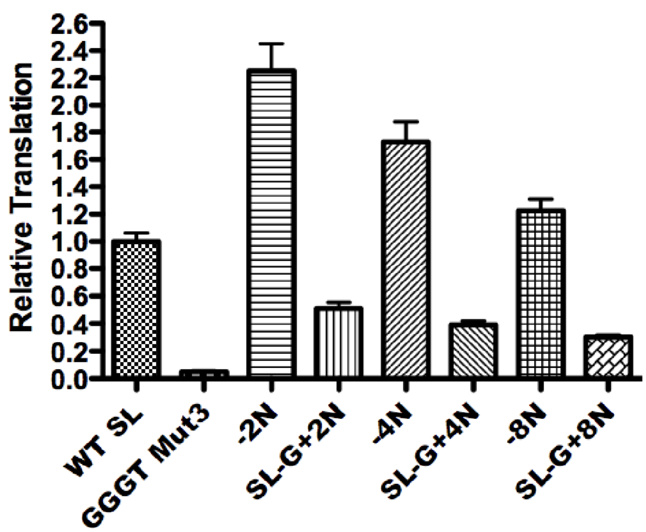


```
                          SL                          ATG
WT       G--------GTTTAATTACCCAAGTTTGAGGGCTAGCCACCATG
-2N      G--------GTTTAATTACCCAAGTTTGAG--CTAGCCACCATG
SL-G+2N  GNN------GTTTAATTACCCAAGTTTGAG--CTAGCCACCATG
-4N      G--------GTTTAATTACCCAAGTTTGAG----AGCCACCATG
SL-G+4N  GNNNN----GTTTAATTACCCAAGTTTGAG----AGCCACCATG
-8N      G--------GTTTAATTACCCAAGTTTGAG--------ACCATG
SL-G+8N  GNNNNNNNNGTTTAATTACCCAAGTTTGAG--------ACCATG
```

A

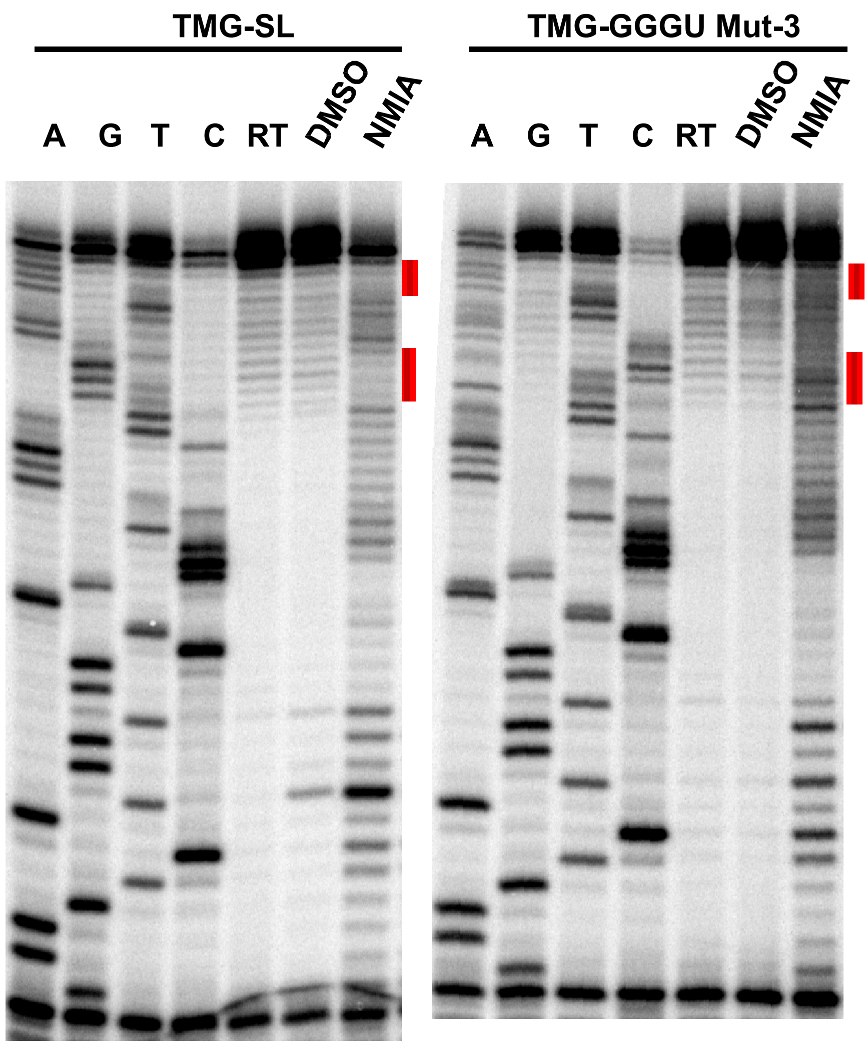

	1 2 3 4 5 6 7 8 9 10 11 12 13 14 15 16 17 18 19 20 21 22
TMG-SL:	TMGpppG-G-U-U-U-A-A-U-U-A-C-C-C-A-A-G-U-U-U-G-A-G
TMG-GGGU Mut3:	TMGpppG-G-U-U-U-A-A-U-U-G-G-G-U-A-A-G-U-U-U-G-A-G

B

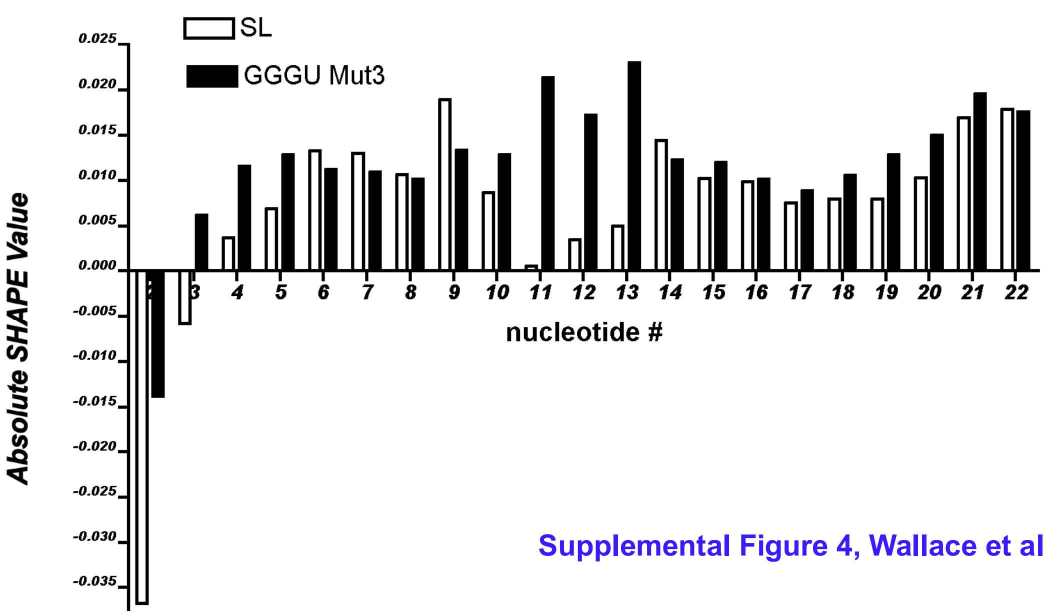

Supplemental Figure 4, Wallace et al.

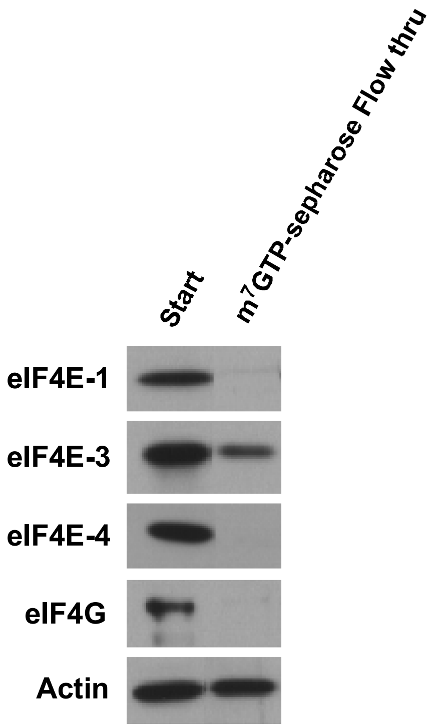

Supplemental Figure 5, Wallace et al.

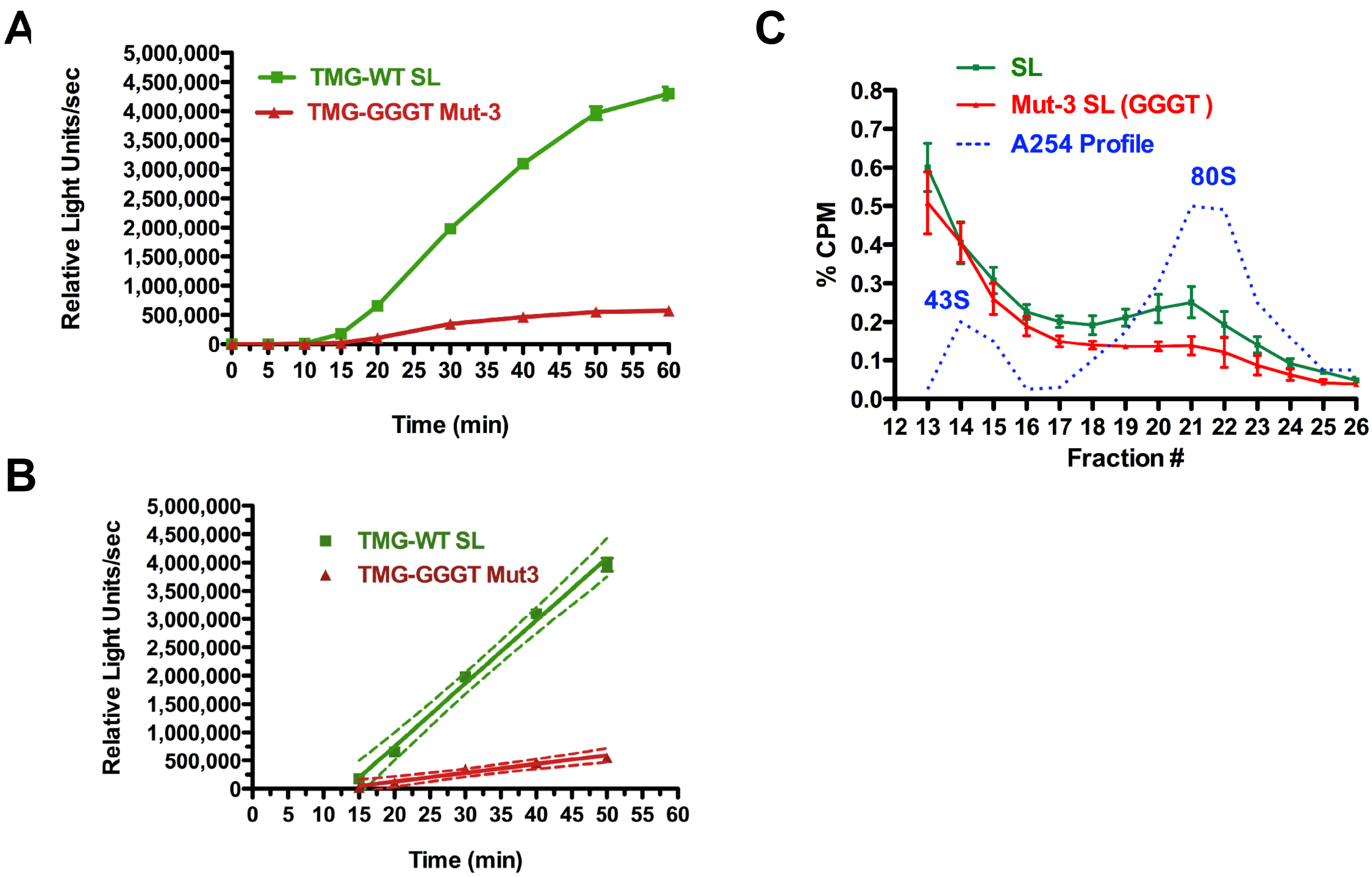

Supplemental Figure 6, Wallace et al.

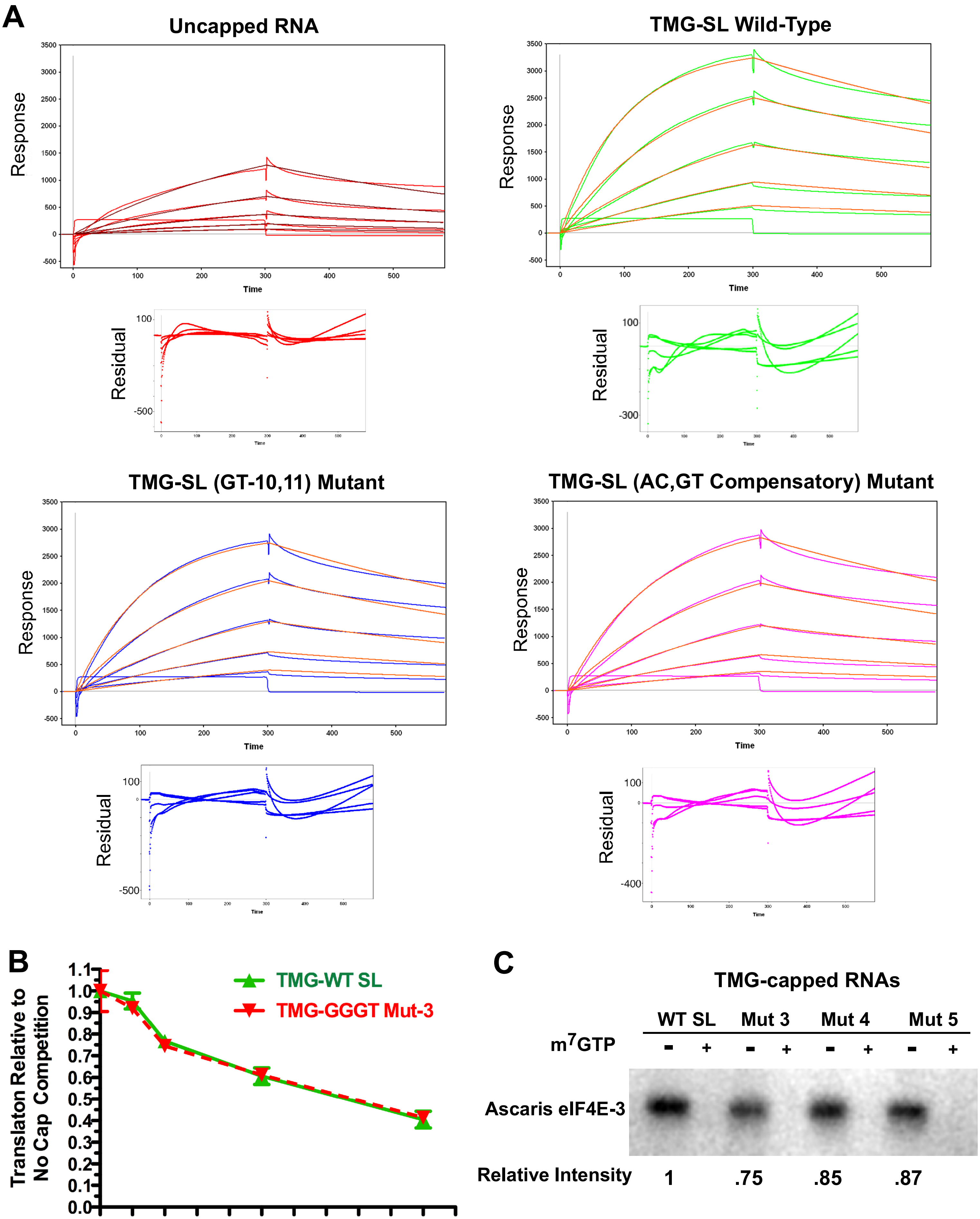

Supplemental Figure 7, Wallace et al.

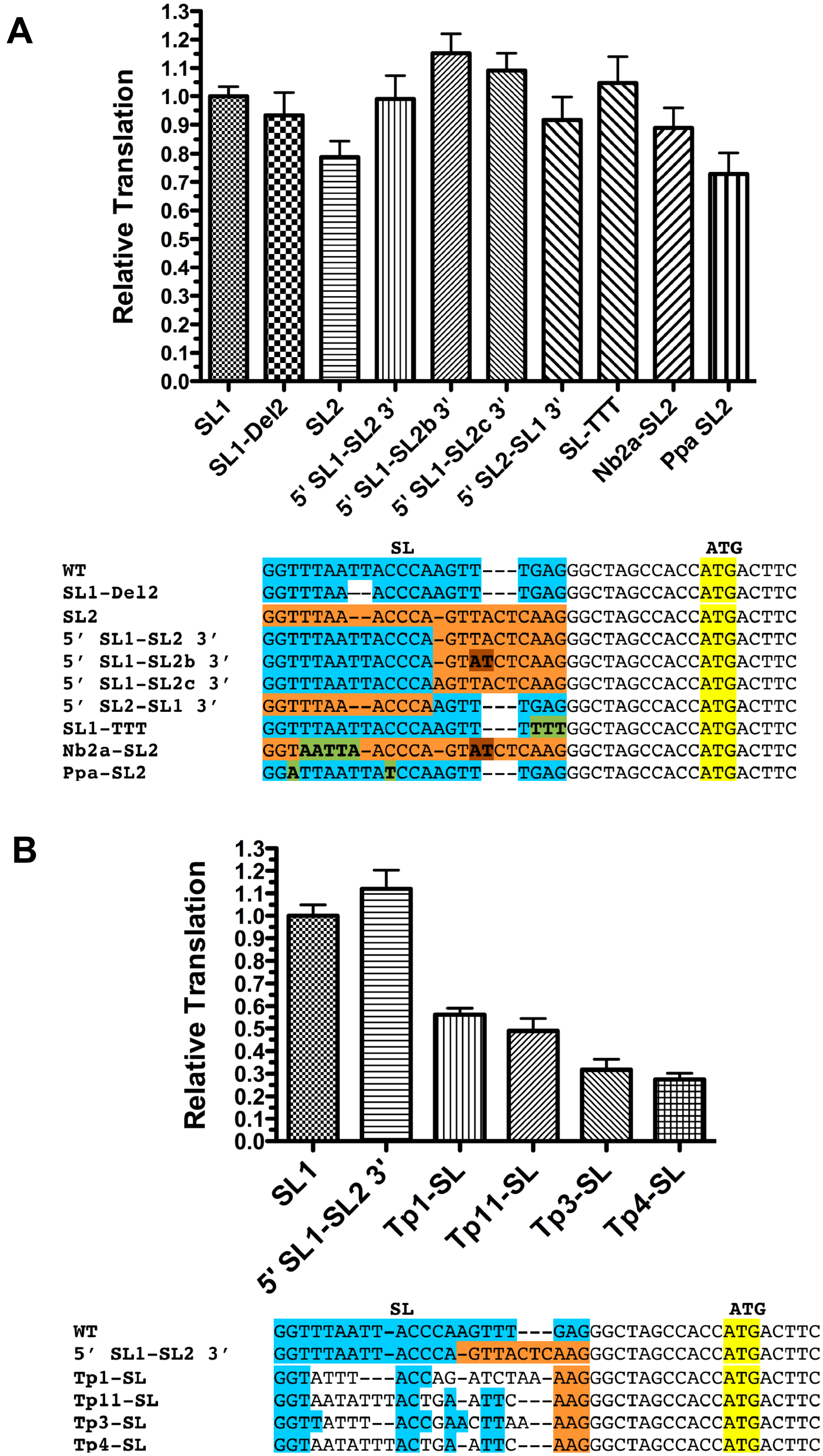

Supplemental Figure 8, Wallace et al.